

# LEPTON SCATTERING ON NUCLEI AT $x > 1$ AND THE NUCLEON SPECTRAL FUNCTION

P. Fernández de Córdoba, E. Marco, H. Müther, E. Oset and A. Faessler

*Institut für Theoretische Physik, Universität Tübingen, 72076 Tübingen, Germany*

## Abstract

We analyze the processes of deep inelastic and quasielastic scattering in the region of  $x > 1$ . These processes are found to be very sensitive to the information contained in the nucleon spectral function in nuclei, particularly to the correlations between energy and momentum. Calculations are done using two spectral functions for nuclear matter and one for finite nuclei,  $^{16}\text{O}$ . Several approximations are also analyzed and are shown to be inaccurate in this region. These results stress the fact that the region of  $x > 1$  contains important information on nuclear dynamical correlations.

## 1 Introduction

Deep inelastic scattering (DIS) and quasielastic scattering (QES) on nuclei at  $x > 1$  (being  $x$  the Bjorken variable) are a very interesting tool to explore nuclear dynamics. In DIS on a free nucleon at rest, the possible values of  $x$  are limited,  $0 < x < 1$ , and in QES the value is fixed,  $x = 1$ . DIS and QES on a nucleus at  $x > 1$  are possible due to the Fermi motion of the nucleons and the interactions between them.

After the discovery of the EMC effect [1], the raise of the ratio of the nuclear structure function to the free one at  $x$  close to 1 was soon identified [2] as the effect of the Fermi motion of the nucleons. This motivated people to investigate the region of  $x > 1$  [2–5], noting that a non vanishing value of the structure function for  $x > 1 + k_{\text{F}}/M$  (with  $k_{\text{F}}$  the Fermi momentum), would require a tail in the momentum distribution,  $n(\vec{p})$ , for  $k > k_{\text{F}}$ . This is indeed the case when the effects of a residual  $NN$  interaction are considered, leading to a correlated many-body system of fermions.

However, it is very dangerous to use only the momentum distributions, because in this region it is essential to take into account the correlations between energy and momentum, which are described by the spectral functions.

In our work [6], we have used two different spectral functions for nuclear matter and one for  $^{16}\text{O}$  in order to quantify the uncertainties of the many-body approach. We have used the theoretical framework developed in Ref. [7], in which nucleons are treated in a relativistic formalism. We have also analyzed several approximations widely used in the calculations of the EMC effect.

We compare our results with the high  $Q^2$  data ( $Q^2 > 60 \text{ GeV}^2$ ) of BCDMS [8], in which DIS dominates and with the low  $Q^2$  data ( $Q^2 \sim 1.3 \text{ GeV}^2$ ) obtained at SLAC [9], in which QES is very important.

## 2 Formalism for inelastic lepton scattering

In our work in Ref. [7], it is shown that using the relativistic formalism we can write the hadronic tensor for a nucleus as

$$W_A^{\prime\mu\nu} = 4 \int d^3r \int \frac{d^3p}{(2\pi)^3} \frac{M}{E(\vec{p})} \int_{-\infty}^{\mu} dp^0 S_h(p^0, p) W_N^{\prime\mu\nu}(p, q), \quad (1)$$

where  $q$  is the virtual photon momentum,  $W_N^{\prime\mu\nu}(p, q)$  is the average of the hadronic tensor for protons and neutrons and  $S_h(p^0, p)$  is the relativistic hole spectral function, normalized as

$$4 \int d^3r \int \frac{d^3p}{(2\pi)^3} \int_{-\infty}^{\mu} d\omega S_h(\omega, p; \rho(r)) = A \quad (2)$$

in symmetric nuclear matter, where  $\mu$  is the chemical potential. Had we used a nonrelativistic formalism, we would have obtained an expression similar to (1) but without the factor  $M/E(\vec{p})$  and evaluated using a nonrelativistic spectral function.

Gauge invariance imposes the following structure of the hadronic tensor in terms of two invariant structure functions  $W_1, W_2$ ,

$$W^{\prime\mu\nu} = \left( \frac{q^\mu q^\nu}{q^2} - g^{\mu\nu} \right) W_1 + \left( p^\mu - \frac{p \cdot q}{q^2} q^\mu \right) \left( p^\nu - \frac{p \cdot q}{q^2} q^\nu \right) \frac{W_2}{M^2}. \quad (3)$$

Since it is customary to show the experimental data for  $W_2$ , we use Eqs. (1) and (3) to write  $W_{2A}$  in terms of  $W_{2N}$  by eliminating  $W_1$ . This is easily accomplished by using the expressions for  $W^{\prime xx}$  and  $W^{\prime zz}$  and taking  $q$  in the  $z$  direction, as usually done. We get

$$W_{2A} = -\frac{q^2}{|\vec{q}|^2} \sum_{p,n} 2 \int d^3r \int \frac{d^3p}{(2\pi)^3} \frac{M}{E(\vec{p})} \int_{-\infty}^{\mu} dp^0 S_h(p^0, p) \times \left[ (p^x)^2 - \frac{q^2}{q} \left( p^z - \frac{p \cdot q}{q^2} |\vec{q}| \right)^2 \right] \frac{W_{2N}(p, q)}{M^2}, \quad (4)$$

where we have substituted a factor 2 of isospin in Eq. (1) by the explicit sum over protons and neutrons.

In the Bjorken limit,  $q^0 \rightarrow \infty$ ,  $-q^2 \rightarrow \infty$ , we define

$$x = \frac{-q^2}{2Mq^0}; \quad x_N = \frac{-q^2}{2p \cdot q} \quad (5)$$

and we find

$$F_{2A}(x) = \sum_{p,n} 2 \int d^3r \int \frac{d^3p}{(2\pi)^3} \frac{M}{E(\vec{p})} \int_{-\infty}^{\mu} d\omega S_h(\omega, p) \frac{x}{x_N} F_{2N}(x_N), \quad (6)$$

where  $F_{2N}(x)$  is the nucleon structure function (which depends smoothly on  $Q^2$ ). This is the expression found in [7] for the  $F_{2A}(x)$  structure function in the Bjorken limit.

For the quasielastic contribution to the structure function,  $W_{2A}^Q$ . Following the steps of Section 3 of Ref. [7] we can write

$$W_A^{\prime\mu\nu} = \sum_{n,p} 2 \int d^3r \int \frac{d^3p}{(2\pi)^3} \frac{M}{E(\vec{p})} \int_{-\infty}^{\mu} S_h(p^0, p) dp^0$$

$$\frac{M}{E(\vec{p} + \vec{q})} \sum_{s_i} \sum_{s_f} \langle p + q | J^\mu | p \rangle \langle p | J^\nu | p + q \rangle^* \delta(q^0 + p^0 - E(\vec{p} + \vec{q})), \quad (7)$$

where

$$\langle p' | J^\mu | p \rangle = \bar{u}(\vec{p}') \left[ F_1(q) \gamma^\mu + i \frac{F_2(q)}{2M} \sigma^{\mu\nu} q_\nu \right] u(p). \quad (8)$$

$W_{2A}^Q$  is given by means of Eq. (3) for the nucleus at rest by

$$W_{2A}^Q = \left( \frac{q^2}{\vec{q}^2} \right)^2 W_{A,Q}^{'00} - \frac{q^2}{\vec{q}^2} W_{A,Q}^{'xx}. \quad (9)$$

By means of Eqs. (7) and (9) we can evaluate the quasielastic structure function  $W_{2A}^Q$ , and express it using the Sachs form factors  $G_E$ ,  $G_M$  [10], defined as

$$G_E(q) = F_1(q) + \frac{q^2}{4M^2} F_2(q),$$

$$G_M(q) = F_1(q) + F_2(q). \quad (10)$$

### 3 The nucleon spectral function in nuclear matter and finite nuclei

We have used three different approaches to evaluate the spectral function: two evaluated for nuclear matter and used by means of the local density approximation and one for the nucleus of  $^{16}\text{O}$ .

#### 3.1. Semiphenomenological approach in nuclear matter

This model is described in detail in Ref. [11]. It evaluates the nucleon self-energy diagrams in a nuclear medium but uses the input from the  $NN$  experimental cross section and the polarization of the  $NN$  interaction to circumvent the use of the  $NN$  potential and the ladder sums. In Ref. [7] it is explained how to include relativistic effects in this spectral function.

#### 3.2. Microscopic approach in nuclear matter

This spectral function has been evaluated using the techniques described in Ref. [12]. The starting point of this many-body calculation is a Brueckner-Hartree-Fock calculation of nuclear matter considering the realistic OBE potential for the  $NN$  interaction.

#### 3.3. Microscopic approach for finite nuclei

The spectral function can be calculated directly for finite nuclei using the procedure described and applied in Ref. [13]. The nucleon spectral function is separated in two parts: the quasiparticle contribution to the spectral function around the quasiparticle pole (the occupied states of the Shell model) and the background contribution which contains the information about the spectral function at energies away from the respective quasiparticle pole. This background contribution,  $S_h^B(\omega, p; \rho(r))$ , is evaluated for nuclear matter,

$$S_{h,A}(\omega, p) = S^{QP}(\omega, p) + 4 \int d^3r S_h^B(\omega, p; \rho(r)). \quad (11)$$

### 3.4. Approximations to be avoided

We have also used several approximations in order to see their accuracy in this region.

i) Non interacting Fermi sea.

The expression used for the spectral function in this approximation is

$$S_h^{UFS}(\omega, p; \rho) = n_{FS}(\vec{p})\delta(\omega - E(\vec{p}) - \Sigma), \quad (12)$$

where  $n_{FS}(\vec{p})$  is the occupation number, 0 for momenta above the local Fermi momentum and 1 for momenta below the local Fermi momentum.  $\Sigma$  is the self-energy which accounts for the binding of the nucleons.

ii) Momentum distribution

Since large momentum components are needed to generate  $F_{2A}(x)$  at  $x > 1$ , one is tempted to use Eq. (12) but using the realistic momentum distribution as an improvement over the previous approximation. The momentum distribution is given by

$$n_I(\vec{p}) = \int_{-\infty}^{\mu} S_h(\omega, p)d\omega. \quad (13)$$

iii) Momentum distribution and the corresponding mean value of the energy

Finally we consider an approximation in which we take for the spectral function the momentum distribution of Eq. (13) but for the value of the energy in the  $\delta$  function we take the mean value of the energy,

$$S_h^{MED}(\omega, p; \rho) = n_I(\vec{p})\delta(\omega - \langle\omega(\vec{p})\rangle). \quad (14)$$

In Fig. 1 we can see the mean value of the energy as a function of  $|\vec{p}|$ . This figure shows that there is an important correlation between the momenta and the mean value of the energy for the bound nucleons. All approximations of Sect. 3.4 lack this correlation and it will be shown that they give wrong results because of that.

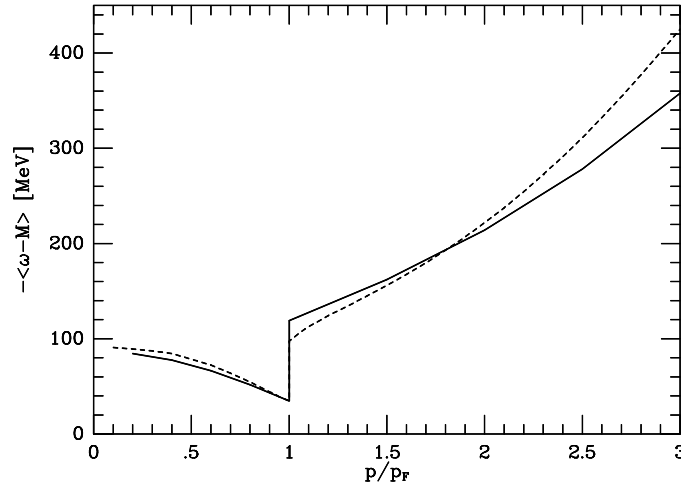


Figure 1: Mean value of the energy of the nucleons as a function of  $|\vec{p}|$ , at  $\rho = \rho_0$ . Solid line: microscopic model [12]; dashed line: semiphenomenological model [11].

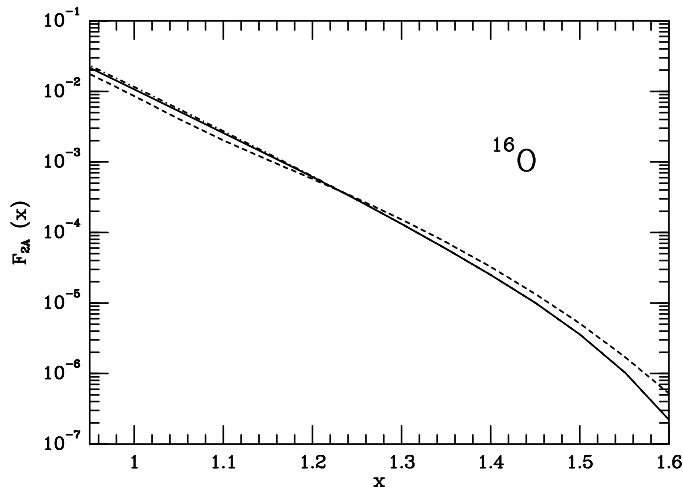


Figure 2: Results obtained for the structure function of  $^{16}\text{O}$ . Solid line: microscopic nuclear matter model [12]; dot-dashed line: microscopic finite nuclei model [13]; dashed line: nonrelativistic semiphenomenological model [11].

## 4 Results

In Fig. 2 we show the results for  $F_{2A}(x)$  calculated with the three different spectral functions introduced in Sects. 3.1–3.3, for the case of  $^{16}\text{O}$ . Since the microscopic nuclear matter and finite nuclei approaches are nonrelativistic, we have also taken the nonrelativistic version of the semiphenomenological approach. The experimental values for  $F_{2N}(x)$  are taken from Ref. [14]. The results obtained with the two spectral functions for nuclear matter (solid line and dashed line) are rather similar. At  $x \simeq 1$  the microscopic spectral function provides results about 20 % higher than the semiphenomenological one. At values of  $x \simeq 1.22$  the two approaches coincide and for  $x \simeq 1.5$ , the semiphenomenological approach provides values of  $F_{2A}(x)$  about 40 % larger than the microscopic one.

The results obtained with the spectral function for finite nucleus, Sect. 3.3, are represented by the dot-dashed line in Fig. 2. They should be compared with those displayed by the solid line since the background contribution to Eq. (11) is obtained from the same nuclear matter result. At  $x \simeq 1$  the results with the spectral function of the finite nucleus are about 8 % higher than with the nuclear matter approach. The differences become smaller as  $x$  increases and for values of  $x \simeq 1.5$  the two approaches give the same results. This latter fact is telling us that at large values of  $x$  one is getting practically all contributions from the background part of the spectral function and none from the quasiparticle part.

In Fig. 3 we show the results obtained with the semiphenomenological approach using the relativistic and nonrelativistic formalisms. The relativistic corrections induce a reduction of 25 % around  $x = 1$  and roughly reduce the structure function  $F_{2A}(x)$  to one half of the nonrelativistic results at  $x \simeq 1.5$ . The effects are so important because we get the contribution from the components of high momentum.

Results obtained for  $F_{2A}(x)$  using the different approximations discussed in Sect. 3.4 are displayed in Fig. 4. The dot-dashed line represents the non interacting Fermi sea,

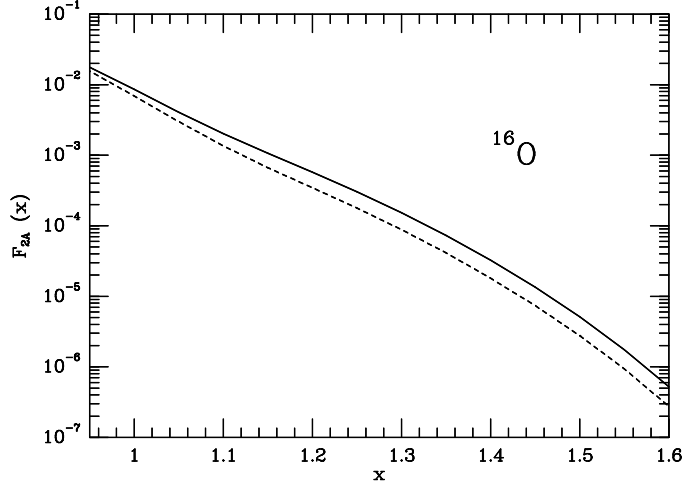


Figure 3: Results obtained for the structure function of  $^{16}\text{O}$  using the semiphenomenological model [11]. Solid line: nonrelativistic formalism; dashed line: relativistic formalism.

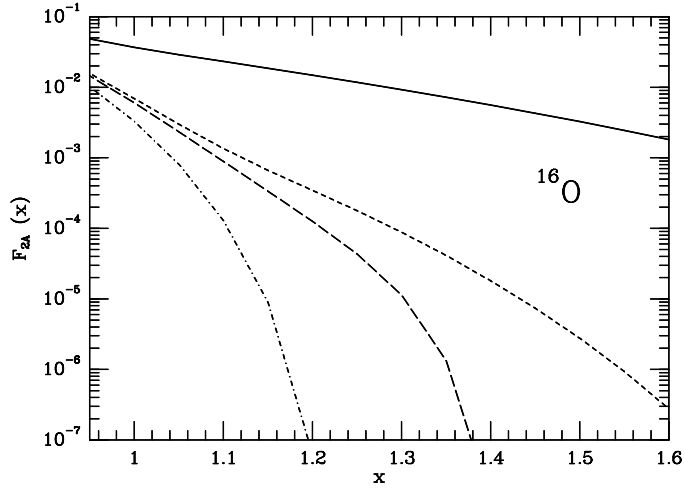


Figure 4: Results obtained for the structure function of  $^{16}\text{O}$  using different approximations. Dot-dashed line: non interacting Fermi sea, Eq. (12); solid line: momentum distribution, Eq. (13); long-dashed line: momentum distribution of the correlated Fermi sea and average energy  $\langle\omega(\vec{p})\rangle$ , Eq. (14); short-dashed line: spectral function, [11].  $Q^2 = 5 \text{ GeV}^2$ .

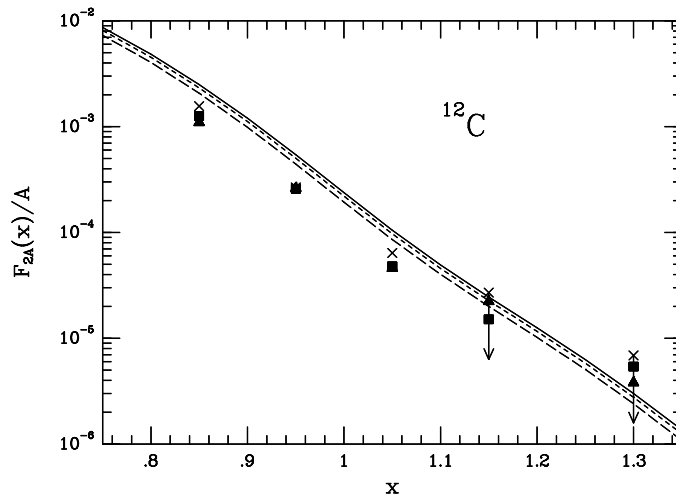


Figure 5: Results for the structure function of  $^{12}\text{C}$  at  $Q^2 = 61, 85$  and  $150 \text{ GeV}^2$  (solid, short-dashed and long dashed lines respectively). The data are from Ref. [8] crosses for  $61 \text{ GeV}^2$ , squares for  $85 \text{ GeV}^2$  and triangles for  $150 \text{ GeV}^2$ . The data for the two largest values of  $x$  are upper bounds.

Eq. (12). We can see that at  $x \simeq 1$  it already provides a structure function of around a factor two smaller than the one obtained with the proper spectral function (short-dashed line). At higher values of  $x$ , the differences are bigger, showing clearly that one is exploring the region of large momenta, above the Fermi momentum, which are not accounted for by the non interacting Fermi sea. Another approximation corresponds to using the realistic momentum distribution  $n_I(\vec{p})$  of Eq. (13) and associating an energy to each  $\vec{p}$  given by its kinetic energy plus a potential, Sect. 3.4 ii). The results (solid line) are outrageously wrong. This demonstrates that the naive use of a momentum distribution, although calculated in a realistic way, may lead to results which are worse than those obtained for an uncorrelated system, if one does not treat the energy-momentum correlation properly. The results obtained using the momentum distribution and the mean value of the energy are shown in the curve with long dashes. This is the better approximation, although the discrepancies with the exact results are still large enough to discourage it too.

In Fig. 5 we see the comparison of our predictions (using the  $Q^2$  dependent structure function of [15]) to the measurements done at  $Q^2 = 61, 85$  and  $150 \text{ GeV}^2$  in Ref. [8]. The agreement with the data is qualitative, the slope is well reproduced but the theoretical results are in average 40 % higher than experiment up to  $x \simeq 1.05$ . At  $x \simeq 1.15$  and  $1.3$  there are only upper bounds which are compatible with our predictions.

In Fig. 6 we can see the results obtained at low values of  $Q^2$  ( $Q^2 = 1.27 \text{ GeV}^2$  at  $x = 1$ ). In this region we include the quasielastic contribution of Eq. (9) and the inelastic contribution, Eq. (4). For low values of  $Q^2$  we use a parametrization of the structure functions [2, 16] where there is a part corresponding to the excitation of the low lying resonances (usually called the inelastic part) and a smooth part for the excitation in the continuum which would stand for the deep inelastic part. We can see that the quasielastic contribution is dominant in all the range of the figure and peaks around  $x = 1$ . The spread of the quasielastic contribution is due to Fermi motion and binding. The inelastic

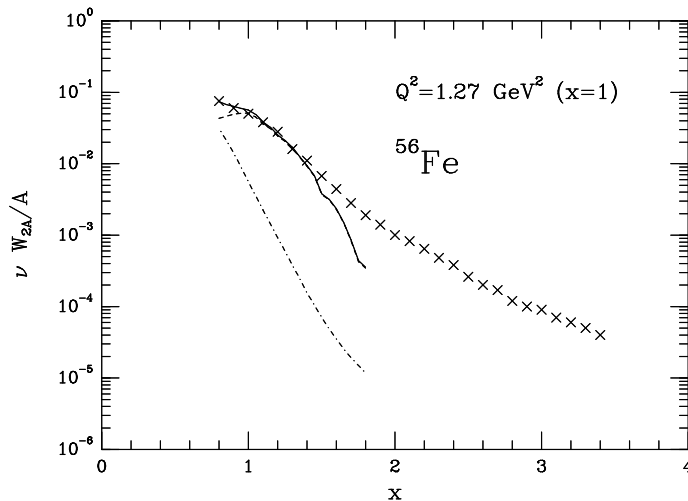


Figure 6: Results for the structure function for  $^{56}\text{Fe}$  at  $Q^2 = 1.27 \text{ GeV}^2$  when  $x = 1$ . Dot-dashed line: inelastic contribution; dashed line: quasielastic contribution; solid line: total contribution.

contribution is small in all the range of the figure compared to the quasielastic contribution. However, at values of  $x < 1$  the inelastic contribution dominates. For values of  $x > 1$  the strength of the structure function is completely dominated by the quasielastic contribution. The agreement with the experiment is rather good up to values of  $x$  around 1.4, from there on our results start diverging from the data.

## 5 Conclusions

We have investigated the region of  $x > 1$  and shown that it provides information on the dynamical properties of nuclei beyond the approximate shell model structure. In order to study these correlations it is important to go to high values of  $Q^2$ , since at low values the quasielastic contribution dominates and it is not so sensitive to the nuclear correlations.

We have seen that in order to treat correctly these correlations, it is important to use spectral functions, without indulging in any approximation. Moreover, since the contribution in this region comes from high momentum components, relativistic effects should be taken into account in the spectral function.

## References

- [1] E.M. Collaboration, J.J. Aubert al., Phys. Lett. B123 (1983) 275.
- [2] A. Bodek and J.L. Ritchie, Phys. Rev. D23 (1981) 1070.
- [3] S.V. Akulinichev and S. Shlomo, Phys. Rev. C33 (1986) 1551.
- [4] H. Araseki and T. Fujita, Nucl. Phys. A439 (1985) 681.
- [5] K. Saito and T. Uchiyama, Z. Phys. A322 (1985) 299.



- [6] P. Fernández de Córdoba, E. Marco, H. Müther, E. Oset and A. Faessler, Nucl. Phys. A, in print.
- [7] E. Marco, P. Fernández de Córdoba and E. Oset, Nucl. Phys. A in print.
- [8] A. C. Benvenuti et al., Z. Phys. C63 (1994) 29.
- [9] B.W. Filippone et al., Phys. Rev. C45 (1992) 1582.
- [10] E. Amaldi, S. Fubini and G. Furland, Pion electroproduction, Springer tracts in modern Physics, 83 (1979), Springer, Berlin.
- [11] P. Fernández de Córdoba and E. Oset, Phys. Rev. C46 (1992) 1697.
- [12] H. Müther, G. Knehr and A. Polls, Phys. Rev. C52 (1995) 2955.
- [13] H. Müther, A. Polls and W.H. Dickhoff, Phys. Rev. C51 (1995) 3040.
- [14] J.J. Aubert et al., Phys. Lett. B114 (1982) 291.
- [15] D.W. Duke and J.F. Owens, Phys. Rev. D30 (1984) 49.
- [16] S. Stein et al., Phys. Rev. D12 (1975) 1884.